Fast-responsive hydrogel as an injectable pump for rapid on-demand fluidic flow control

Rongcong Luo,[1] Ngoc-Duy Dinh,[1] and Chia-Hung Chen[1,2,3,a]
[1]*Department of Biomedical Engineering, National University of Singapore,*
21 Lower Kent Ridge Road, Singapore 119077
[2]*Singapore Institute of Neurotechnology (SINAPSE), National University of Singapore,*
21 Lower Kent Ridge Road, Singapore 119077
[3]*Biomedical Institute for Global Health Research & Technology (BIGHEART),*
National University of Singapore, 21 Lower Kent Ridge Road, Singapore 119077

Chemically synthesized functional hydrogels have been recognized as optimized soft pumps for on-demand fluidic regulation in micro-systems. However, the challenges regarding the slow responses of hydrogels have very much limited their application in effective fluidic flow control. In this study, a heterobifunctional crosslinker (4-hydroxybutyl acrylate)-enabled two-step hydrothermal phase separation process for preparing a highly porous hydrogel with fast response dynamics was investigated for the fabrication of novel microfluidic functional units, such as injectable valves and pumps. The cylinder-shaped hydrogel, with a diameter of 9 cm and a height of 2.5 cm at 25 °C, achieved a size reduction of approximately 70% in less than 30 s after the hydrogels were heated at 40 °C. By incorporating polypyrrole nanoparticles as photothermal transducers, a photo-responsive composite hydrogel was approached and exhibited a remotely triggerable fluidic regulation and pumping ability to generate significant flows, showing on-demand water-in-oil droplet generation by laser switching, whereby the droplet size could be tuned by adjusting the laser intensity and irradiation period with programmable manipulation. *Published by AIP Publishing.* [http://dx.doi.org/10.1063/1.4983493]

I. INTRODUCTION

Devices for manipulating fluidic flows with on-demand control for biomedical and industrial applications have received increased attention, and a variety of technologies, such as electrics,[1] optics,[2] acoustics,[3] and mechanics,[4] have been investigated to achieve on-demand fluidic flow control in micro-channels. However, most of these methods require complicated experimental approaches, which increases cost while decreasing flexibility. Moreover, due to their solid mechanical properties, these devices cannot be directly injected into a micro-system, representing a limitation in biomedical applications.

Recently, a chemically synthesized stimulus-responsive hydrogel was developed that can be easily injected into a micro-system, as a soft pump to control fluid flows at a micro-scale.[5,6] In response to stimulation, functional hydrogels absorb aqueous solutions during the swelling process and expel them during contraction. Accordingly, a wide range of desirable valves,[7] pumps,[8] and fluidic oscillators[9] have been designed and fabricated using functional hydrogels. However, the slow response and mechanical weakness of stimulus-responsive hydrogels are the main barrier to utilizing them for rapid reagent release,[10,11] actuator fabrication,[5,12] on/off microfluidic switches,[13] and effective pumping components.[14]

The slow responsive kinetics of hydrogels primarily result from the inherent constraints associated with the synthesis method. Conventionally, hydrogels are synthesized from monomer

a)Author to whom correspondence should be addressed: biecch@nus.edu.sg. Tel. +(65) 6516-1624. Department of Biomedical Engineering, National University of Singapore, 9 Engineering Drive 2, Block E1-05-27, Singapore 117578.

solutions via radical polymerization, a general-purpose method for producing synthetic hydrogels. Although this method is commonly used, it generates hydrogels containing a homogeneous nano-porous network, which critically slows vitrification during the shrinking/swelling process and limits the response speed of hydrogels.[15–17] Although efforts to enhance response kinetics have been made by synthesizing thin gel membranes,[18,19] incorporating porogens,[20] grafting dangling chains,[21] or hybridizing nanoparticles within the polymeric network,[22] the challenge of optimizing response speed and mechanical stability remains. Indeed, no methods for fabricating a fast stimulus-responsive hydrogel with a rapid response time for effective fluidic pumping and control have been established, primarily because there are no reported techniques for designing an ideal hydrogel network combining many favorable factors, such as a macro-porous structure,[23] a flexible hydrogel network chain,[24] and a reaction-site enriching domain[25] that synergistically and cooperatively enhances the hydrogel's dynamic response to stimuli. Although in previous work, a 4-hydroxybutyl acrylate (4HBA)-enabled one-step hydrothermal process was applied to generate a gradient porous hydrogel with an effective stimulus response, the pumping efficiency was limited by its gradient porous structure, in terms of squeezing out small amounts of water from the dense porous side.[26]

Herein, we report a method for producing a thermally and optically responsive hydrogel with a fast response to temperature or laser stimulation. The procedure was based on heterobifunctional crosslinker-enabled two-step hydrothermal phase separation,[26,27] which was achieved using a heterobifunctional crosslinker that first linked to the pre-gel monomers to form pre-gel polymer chains with reactive side groups at 70 °C. The polymer chains were then treated at a higher temperature of 180 °C to induce phase separation and form covalent bonds between the polymer chain aggregates, thereby producing a macro-porous three-dimensional hydrogel with a flexible network chain and a polymer-rich domain.

These favorable features synergistically endowed the hydrogel with fast responsiveness at a centimeter scale (supplementary material 1), enabling the hydrogel to generate a strong ejection force, pushing fluid in a certain direction. Therefore, through integration of polypyrrole (PPy) nanoparticles as photothermal transducers, a novel injectable photo-responsive hydrogel pump for generating water-in-oil droplets in an on-demand manner in a micro-system via programmable laser irradiation (to increase the hydrogel's temperature to ∼40 °C) was fabricated, which has been difficult to achieve using previously reported methods.[28–32]

II. METHODS AND MATERIALS

A. Hydrothermal phase separation

Our one-pot, two-step sequential hydrogelation strategy for generating a fast-responsive hydrogel is schematically illustrated in Fig. 1. In the first step, N-isopropylacrylamide (NIPAM) and 4-hydroxybutyl acrylate (4HBA) were dissolved in deionized water (DI H$_2$O), which was subsequently loaded into a hydrothermal reactor and heated at 70 °C for 10 h. During this reaction step, NIPAM was polymerized with 4HBA via hydrothermally induced free radical vinyl polymerization, generating NIPAM polymer chains with pendant hydroxyl groups (PNIPAM-OH). After the reaction, the obtained PNIPAM-OH was purified via dialysis to remove unreacted monomers and then lyophilized. Next, PNIPAM-OH was dissolved in DI H$_2$O and heated in a hydrothermal reactor at 40 °C for 1 h to precipitate the PNIPAM-OH polymers. Immediately following this process, the temperature of the hydrothermal reactor was abruptly increased to 180 °C and maintained at this temperature for 4 h. During this reaction step, the pendant hydroxyl groups of the phase-separated PNIPAM-OH were hydrothermally linked via induced dehydration polymerization, forming a crosslinked porous 3D PNIPAM network. After the reaction, the dehydrated PNIPAM network was peeled off the reactor and rehydrated in DI H$_2$O to form a macro-porous PNIPAM hydrogel.

B. Sample preparation

One gram of NIPAM (Sigma-Aldrich), 100 μl of 4HBA (Polysciences Asia Pacific, Inc.), and 5 mg of ammonium persulfate (APS, Sigma-Aldrich) were dissolved in 10 ml of DI H$_2$O
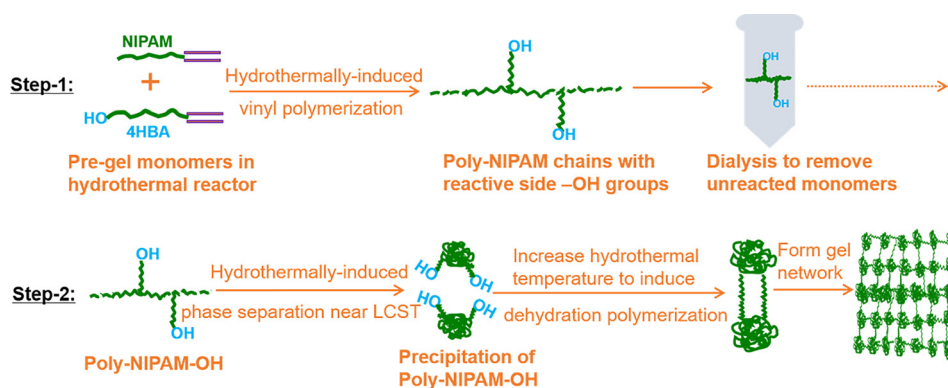
FIG. 1. Schematic representation of the 4HBA-enabled two-step hydrothermal synthesis of the fast-responsive hydrogel.

and then filtered and loaded into a 200 ml hydrothermal reactor (Latech, Singapore). The reactor was subsequently heated in a 70 °C oven for 10 h. After the reaction, the solution was dialyzed in a tube (MWCO 3500) for 4 days to remove unreacted chemicals, and the solution was lyophilized. Next, 500 mg of the lyophilized polymers was dissolved in 5 ml DI H_2O and loaded into the hydrothermal reactor, which was then heated in a 40 °C oven for 1 h. Immediately afterward, the reactor temperature was abruptly increased to 180 °C, which was maintained for 4 h to trigger the dehydration polymerization process. After the reaction, the hydrogel was peeled from the reactor and incubated in 2 l of DI H_2O for one week, with regular changing of H_2O and alternating heating (40 °C)/cooling (25 °C) to fully hydrate the material, forming the 4HBA-based hydrogel.

To prepare a photo-responsive hydrogel, polypyrrole (PPy) nanoparticles were loaded into the 4HBA-based hydrogel as photothermal transducers. The PPy nanoparticles were prepared according to a previously reported procedure.[33] To load PPy, a hydrogel with a diameter of 0.88 cm and a height of 0.25 cm was first compressed to squeeze out excess water, followed by the addition of 400 μl of a PPy nanoparticle solution with a concentration of 5 mg/ml. The hydrogels were subsequently washed thoroughly with water at room temperature for 2 days to remove the loosely bound nanoparticles. The obtained PPy-loaded hydrogel was then suspended in DI H_2O and loaded into a syringe connected to a silicon tube with a diameter of 0.2 cm.

A conventional N, N-methylenebisacrylamide (BIS)-based PNIPAM hydrogel was also prepared using an N, N-methylenebisacrylamide (BIS) crosslinker via radical polymerization of NIPAM monomers. Briefly, 1 g of NIPAM, 25 mg of BIS, and 10 mg of APS were dissolved in 10 ml of H_2O. Subsequently, 1% (v/v) tetramethylethylenediamine (TEMED) was added to this solution, which was then kept at room temperature for 12 h to initiate polymerization. The obtained hydrogel was washed thoroughly by incubation in DI water for 1 week. Structural analysis of both the 4HBA-based hydrogel and the BIS-based hydrogel was performed using a scanning electron microscope (SEM) (JEOLJSM-6430F, JEOL, Japan). Additionally, the frozen hydrogel was lyophilized and sectioned for observation, and hydrogel sections were coated with gold and analyzed via SEM.

III. RESULTS AND DISCUSSION

A. Thermal response of the 4HBA-based hydrogel

The synthesized 4HBA-based hydrogel structure exhibited a remarkably rapid thermal response dynamics. To determine the thermal response time, a cylinder-shaped microporous hydrogel with a diameter of 9 cm and a height of 2.5 cm was prepared and subjected to alternating thermal stimulation. The original cylinder-shaped hydrogel achieved a size reduction of approximately 70% in less than 30 s after the hydrogels were heated at 40 °C [Fig. 2(a), Multimedia view: Video-1]. To illustrate this improvement, we fabricated a hydrogel with an identical diameter and height, using a conventional N, N-methylenebisacrylamide (BIS)
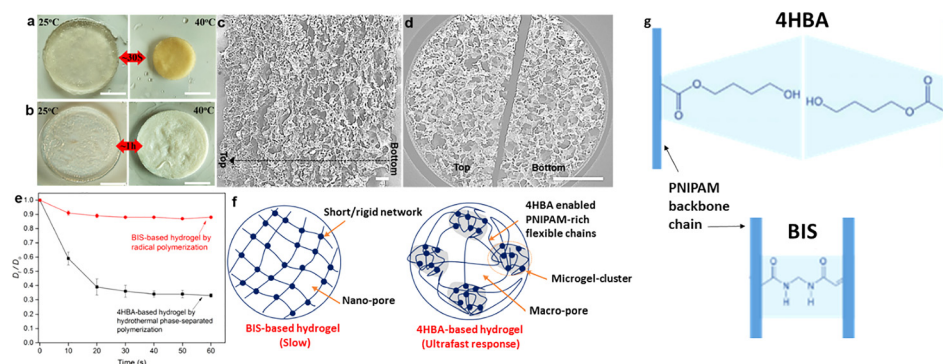
FIG. 2. Size change and thermal-responsive behavior of (a) our 4HBA-crosslinked hydrogel produced via the hydrothermal synthesis route (Video-1) and (b) a conventional BIS-crosslinked hydrogel produced via radical polymerization; scale bar, 3 cm (Video-2). (c) SEM view of a cross-section of the hydrogel; scale bar, 200 μm. (d) SEM image showing the morphology of top and bottom surfaces of the hydrogel; scale bar, 1 mm. (e) Evolution of the size of 4HBA-crosslinked and BIS-crosslinked hydrogels after a temperature increase from 25 °C to 40 °C. For each type of hydrogel sample, three specimens were tested to obtain the mean value and standard deviation for each data point. (f) Schematic illustration of the mechanism underlying the fast-responsive kinetics of the 4HBA-crosslinked hydrogel produced via the hydrothermal synthesis route. (g) Schematic illustration of the chemical structure of 4HBA-based hydrogels and BIS-based hydrogels. Due to the long distance between the PNIPAM backbone chains, a highly porous network in a 4HBA-based hydrogel can be obtained, showing an ultrafast response to thermal stimuli. (Multimedia view) Video-1 [URL: http://dx.doi.org/10.1063/1.4983493.1], Video-2 [URL: http://dx.doi.org/10.1063/1.4983493.2]

crosslinker via radical polymerization. The changes in the size of the 4HBA hydrogel and BIS hydrogel due to increasing the temperature from 25 °C to 40 °C were recorded. The conventional BIS-based hydrogel shrunk slowly when the temperature was increased to 40 °C, requiring more than 1 h to reach equilibrium [Fig. 2(b), Multimedia view: Video-2].

In contrast, the 4HBA-based hydrogel shrunk rapidly at a temperature higher than its lower critical solution temperature (LCST), requiring ∼15 s for the diameter to be reduced by half [Fig. 2(e)]. During this process, the hydrogel undergoes a rapid change in volume, with remarkable mechanical shrinkage in isotropic directions, indicating the aggregation forces operating within the highly porous polymeric network to pump out a large amount of water from the interior of the hydrogel matrix. In contrast, our hydrogel shrunk rapidly to its equilibrium state, requiring ∼15 s for the diameter to be reduced by half. During this process, our hydrogel underwent large, rapid changes in volume, with remarkable mechanical shrinkage, indicating strong aggregation forces operating within the hydrogel matrix. Along with the shrinkage process, trapped water in the hydrogel matrix was rapidly squeezed out from the interior of the hydrogel matrix, suggesting potential for application as a fluid-pumping component.

The fast thermal response dynamics observed in this unique hydrogel was due to its synergetic combination of three important features that cooperatively accelerate the hydrogel response. (1) Due to the well-interconnected pores within the hydrogel, as indicated via SEM [Figs. 2(c) and 2(d)], free water in the water-rich regions was rapidly transferred into the surrounding regions, forming an interconnected water release channel throughout the hydrogel that could facilitate the rapid evacuation of water from the collapsing network, resulting in a fast response rate of the hydrogel. (2) Due to the differences in reactivity between the $CH_2=CH_2$ and -OH groups of the 4HBA crosslinker, a two-step gelation process was applied, enabling the formation of longer PNIPAM chains. Moreover, due to the long alkyl chains of 4HBA, a high degree of freedom and flexibility of the crosslinked PNIPAM chains was achieved. Upon increasing the temperature above the lower critical solution temperature (LCST), the long flexible linear PNIPAM bridge chains shrunk rapidly because no crosslinked restriction existed [Fig. 2(f)]. (3) With the 4HBA crosslinker, the formation of a heterogeneous network of the PNIPAM hydrogel was achieved by applying a hydrothermal process. Compared with the BIS-based hydrogel, containing a dense network with nano-pores, the ABS-based hydrogel contained a highly porous network with micro-pores for an ultrafast response according to thermal stimuli [Fig. 2(g)].

B. Photo-responsive PPy-loaded composite hydrogel

To convert the thermal-responsive hydrogel to a photo-responsive hydrogel, PPy nanoparticles were loaded into the 4HBA-based hydrogel to act as photothermal transducers, thus generating a composite hydrogel, whose contraction/swelling responses to laser irradiation were recorded and are shown in Fig. 3(a). A cylinder-shaped hydrogel with a diameter of 0.88 cm and a height of 0.25 cm suspended in H_2O was successfully injected through a silicon tube with a diameter of 0.2 cm. After injection, the deformed hydrogel rapidly returned to its original, un-deformed volume, as surrounding water was re-absorbed into the hydrogel.

The compression test of the composite hydrogel was performed on a universal testing system (Instron) equipped with a 10 N force transducer in a uniaxial manner at a speed of 1.5 mm/min. The compressive modulus was determined based on the slope of the initial linear region of the stress-strain curve. The compressive stress-strain profiles of the hydrogels after being subjected to different numbers of injections were recorded [Fig. 3(b), Multimedia view: Video-3]. It was found that after 10 cycles of injection, the hydrogel maintained its mechanical properties, such as its compressive modulus ($\sim$5.5 $\pm$ 1.2 kPa). The favorable mechanical stability of the hydrogel was presumably due to the reversible collapsibility of the hydrogel's thick and flexible pore wall structure.[34,35]

After injection, water was collected and subjected to UV-vis-NIR analysis to monitor the PPy nanoparticles remaining within the hydrogel matrix. It was found that the loaded amount of PPy nanoparticles in the hydrogel was gradually reduced with the injection cycle. After 1 cycle of the injection experiment, approximately 25% of the loaded PPy nanoparticles were released from the hydrogel. After 5 cycles of the injection experiment, the reduction of PPy nanoparticles reached a steady state and was maintained at approximately 50% of the original loading amount [Fig. 3(c)]. Although the amount of PPy nanoparticles was decreased by increasing the number of stress cycles, the remaining amount of PPy in the hydrogel matrix after 10 cycles still generated sufficient heat to effectively induce shrinkage of the PNIPAM hydrogels. This observation indicated that a stable amount of PPy remained in the hydrogel matrix after several injection-swelling-injection cycles.
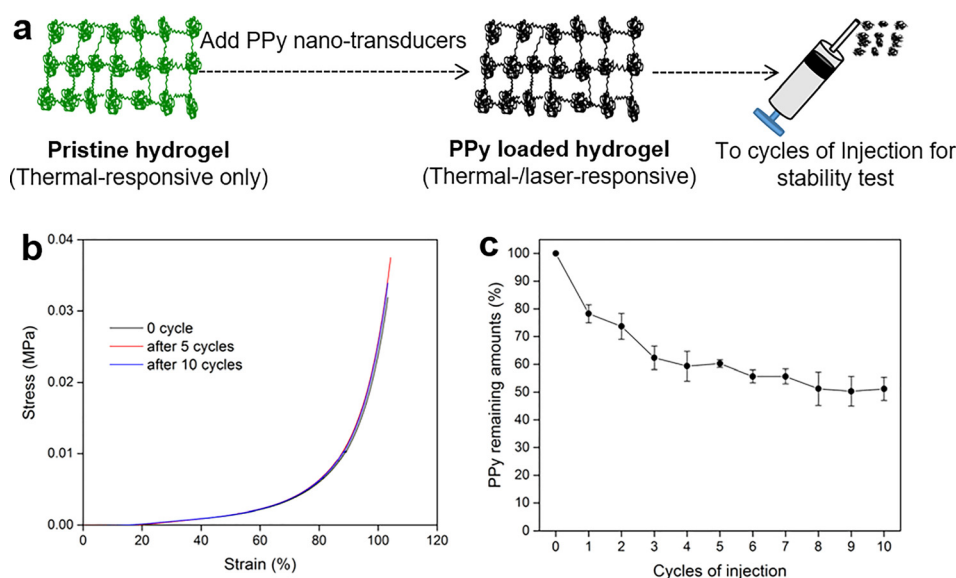

FIG. 3. (a) Schematic representation of the loading of PPy photothermal nanotransducers into the hydrogel, to endow it with a laser-responsive ability and the syringe-based injectability test of the PPy-loaded hydrogel. (b) Compressive stress-strain curves of the original composite hydrogel (0 cycle) and the composite hydrogel after being subjected to 5 cycles and 10 cycles of injection. (c) Amounts of PPy remaining in the composite hydrogel after each cycle of injection. Five hydrogel specimens were tested to obtain the mean value and standard deviation for each data point. (Multimedia view) Video-3 [URL: http://dx.doi.org/10.1063/1.4983493.3]

When correlated with the compressive stress-strain profiles of the composite hydrogel, this result indicated that the incorporation of PPy nanoparticles into the hydrogel through physical interaction did not alter the hydrogel's mechanical properties. The easy injection of the composite hydrogel offers several advantages in the design of a micro-system: (1) the elimination of *in situ* hydrogel fabrication in channels, which requires multiple steps, limits the selection of pre-gel materials, and forms only slow-responsive (~minutes scale) hydrogels;[36,37] (2) the hydrogel can be injected into pre-formed chambers, eliminating the possible adverse effects of the chamber fabrication step (e.g., plasma bonding) on hydrogel performance;[38,39] and (3) the size, shape, and volume of the hydrogel can be conveniently adjusted to the design of the channel, increasing flexibility in terms of fluid channel design and control.[40]

C. Optical triggered fluidic control in a micro-channel

The photo-responses of the PPy-loaded hydrogel were investigated by recording the change in the size of the hydrogel under different conditions of laser irradiation. After being irradiated using a laser (wavelength: 915 nm) with an intensity of 1.45 W/cm^2 for 4 s, the diameter of a cylinder-shaped hydrogel that was originally 0.88 cm in diameter was reduced to approximately 0.55 cm, indicating the superior photo-response speed of the hydrogel. The heat effect and thermal energy distribution according to laser irradiation are summarized in supplementary material 2. The swelling/de-swelling of the hydrogel according to laser switching was highly reversible. The hydrogel exhibited no fatigue phenomena after several cycles of laser irradiation, as indicated by the observation that the hydrogel could be rapidly restored to its original diameter, without any changes, after laser irradiation was switched off [Fig. 4(a)].

To illustrate the applications of this photo-responsive hydrogel for fluidic control, a cylinder-shaped hydrogel with a diameter of 0.88 cm and a height of 0.25 cm was injected through a silicon tube into the pre-formed polydimethylsiloxane (PDMS) chamber with one open end, filled with green-colored water maintained at constant pressure, where the hydrogel was designed to act as laser-responsive pump for water dispensing [Fig. 4(b), Multimedia view: Video-4]. After subjecting the hydrogel pump to laser irradiation (915 nm, 2.55 W/cm^2) for less
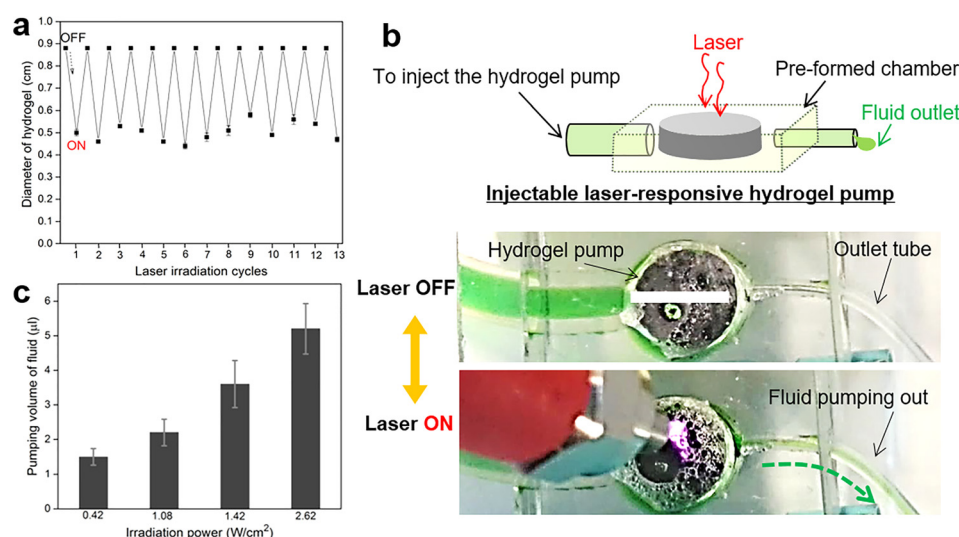

FIG. 4. (a) The laser response dynamics of the PPy-loaded hydrogel determined by recording the change in the size of the hydrogel in response to laser irradiation at 915 nm with an intensity of 1.45 W/cm^2 and a duration of 4 s. (b) Schematic representation and photographs showing that the hydrogel acted as a laser-responsive pump for water dispensing, where switching the applied laser irradiation (915 nm, 2.55 W/cm^2, 1 s) can control the fluid flow; scale bar, 8 mm. (c) Control of the volume of the liquid dispensed by tuning the intensity of laser irradiation received by the hydrogel pump, where the hydrogel pump was irradiated with different intensities of laser irradiation for 10 s. The laser switching cycles were repeated 5 times to obtain the mean value and standard deviation for each data point. (Multimedia view) Video-4 [URL: http://dx.doi.org/10.1063/1.4983493.4], Video-5 [URL: http://dx.doi.org/10.1063/1.4983493.5]

than 1 s, the water was immediately pushed out of the chamber, demonstrating the hydrogel's applicability as a pumping component for liquid dispensing. Laser stimulation provided fine control of the volume of the liquid dispensed by allowing convenient tuning of the intensity of laser irradiation received by the hydrogel pump. The hydrogel pump was irradiated with different intensities of laser irradiation for 10 s, and the volume of the liquid that flowed out was recorded. With an increase in laser irradiation power, a larger volume of the liquid was discharged from the chamber [Fig. 4(c), Multimedia view: Video-5].

D. The hydrogel pump enables on-demand droplet generation

Droplet generation was triggered by laser irradiation of the hydrogel pump. A schematic representation of the hydrogel pump-enabled on-demand droplet generation device is illustrated in Fig. 5(a). There were two channels in the device. One channel consisted of a syringe containing a cylinder-shaped hydrogel with a diameter of 0.88 cm and a height of 0.25 cm, where the syringe was filled with green-colored water at constant pressure. The other channel was filled with silicon oil and surfactant and was connected to a syringe pump with a constant flow rate of 100 μl/min [Fig. 5(b)].
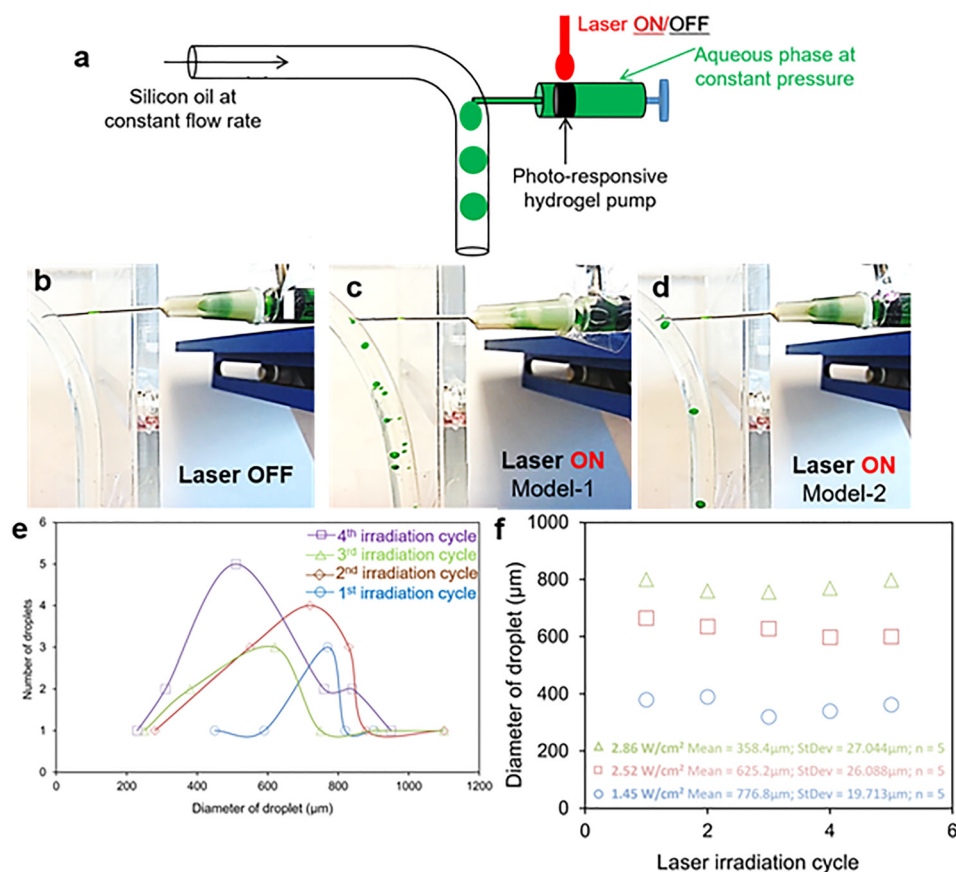

FIG. 5. (a) Schematic representation of the laser-responsive hydrogel pump-enabled droplet generation device, where the source of laser irradiation is fixed above the area of the hydrogel pump. (b) Photograph showing the morphology of the droplet generation device when the laser is in the OFF state; scale bar, 5 mm. (c) The captured image shows the droplets formed by the hydrogel pump operated by irradiating the hydrogel pump at a fixed intensity (1.62 W/cm^2) for 10 s and then switching off the laser (Mode-1) (Video-6). (d) The captured image shows the droplets formed by the hydrogel pump operated by rapidly switching the laser irradiation (in less than 3 s) received by the hydrogel pump between different intensities (Mode-2); this image was captured at a laser intensity of 1.45 W/cm^2 (Video-7). (e) Size distribution of the droplets generated from the same hydrogel pump after being irradiated by 4 cycles of laser stimulation under Mode-1. (f) Mode-2 operation allowed tunability of the diameter of droplets by adjusting the laser irradiation intensity. (Multimedia view) Video-6 [URL: http://dx.doi.org/10.1063/1.4983493.6], Video-7 [URL: http://dx.doi.org/10.1063/1.4983493.7]

Laser irradiation was provided by a continuous wave (CW) laser source with a wavelength of 915 nm and a maximum output power of 8 W (BWT Beijing Ltd. China). The laser intensity was first calculated using the equation $(250/d^2) \times$ Output power, where d is the diameter of the laser beam in millimeters, which was determined using an IR indication card. The output power was determined using a model841-PE power/energy meter (Newport Opto-Electronic Technologies). A cylinder-shaped composite hydrogel with a diameter of 0.88 cm and a height of 0.25 cm was squeezed into a 1 ml syringe filled with green-colored water and maintained at a constant pressure by expelling the entrapped air. The syringe was inserted into a silicon tube with silicon oil flowing at a constant rate of 100 μl/min. The laser irradiation source was positioned above the area of the hydrogel pump and was operated under two modes of control, as follows.

Mode-1 was operated by irradiating the hydrogel pump at a fixed intensity (1.62 W/cm^2) for 10 s and then switching off the laser to evaluate droplet generation. This process was repeated several times to assess the size distribution of droplets generated by the hydrogel pump [Fig. 5(c), Multimedia view: Video-6]. The droplets formed via the operating mode-1 process are shown in Fig. 5(c). A number of droplets with varying diameters were generated by the hydrogel pump after one cycle of laser irradiation. The size distribution of the droplets generated by the same hydrogel pump after 4 cycles of laser stimulation is analyzed in Fig. 5(e). It was found that the droplets generated in the first and second cycles of laser irradiation were nearly monodispersed (∼700 μm in diameter). The droplets generated in the third and fourth cycles of laser irradiation exhibited a wider size distribution (∼500 μm). The decreased diameter of the droplets generated from the hydrogel pump after several irradiation cycles resulted from the partial melting of the PPy nanoparticles due to laser stimulation.[27,37]

Mode-2 was operated by rapidly switching between different intensities of laser irradiation (in less than 3 s) received by the hydrogel pump, with the purpose of reducing PPy melting and generating droplets with a controllable size [Fig. 5(d), Multimedia view: Video-7]. The volume of the generated droplets could be tuned by adjusting the laser irradiation intensity. The droplets generated under this mode exhibited a relatively uniform size distribution, as shown in Fig. 5(f). A higher intensity of laser irradiation triggered a higher photothermal conversion efficiency, causing greater shrinking of the hydrogel pump to generate droplets with a large volume. By controlling the laser irradiation intensity, the diameter of the water droplets could be changed in a programmable manner from approximately 400 μm to 800 μm. Compared with mode-1 operation, the droplet diameter remained in a steady state, without obvious changes, after 5 cycles of laser irradiation under mode-2 operation, indicating that on-demand generation of droplets with a controllable size could be achieved using this hydrogel pump.

To characterize the stability of the hydrogel pump, 15 cycles of laser irradiation were conducted to produce 15 droplets, which were analyzed using image J. The experiment was carried out with a laser intensity of 1.53 W/cm^2, irradiating the hydrogel for 2 s to generate a water-in-oil droplet. The mean diameter of the droplets was 562.5 ± 44.59 μm (supplementary material 4).

IV. CONCLUSIONS

In conclusion, a novel hydrogel with a fast response and easily compressible mechanical properties was synthesized as a functional fluidic component for on-demand fluidic flow control in micro-systems. Due to a highly porous internal structure, the synthesized hydrogels exhibited a remarkable thermal response and shrunk dramatically, inducing significant fluidic flows as an injectable pump. A cylinder-shaped hydrogel with a 9 cm diameter and a 2.5 cm height at 25 °C shrank to ∼70% of its volume within 30 s after heating at 40 °C. Accordingly, a significant inertial aqueous flow was generated to overcome oil-water surface tension and generate water-in-oil droplets on demand. Droplets with a tunable diameter were produced by adjusting the laser irradiation intensity and irradiation time. Moreover, this small injectable hydrogel pump is easy to integrate into a microfluidic system to enrich functionalities and to shrink the entire system's size dramatically. We believe that the use of this novel hydrogel as an injectable pump for rapid on-demand fluidic control will be broadly beneficial to chemists, physicists, material scientists, integrative micro-system designers, and bioengineers alike.

SUPPLEMENTARY MATERIAL

See supplementary material for (1) Comparison of the thermal response and mechanical properties of a hydrothermally phase-separated hydrogel synthesized with 4HBA as a cross-linker with a conventional hydrogel synthesized with BIS as a crosslinker, (2) The heat distribution according to laser irradiation, (3) Distribution of the droplets generated via mode-1 laser operation, and (4) Uniformity of the droplets generated via mode-2 laser irradiation.

ACKNOWLEDGMENTS

[1]B. Daunay, P. Lambert, L. Jalabert, M. Kumemura, R. Renaudot, V. Agache, and H. Fujita, Lab Chip **12**, 361 (2012).
[2]R. M. Lorenz, J. S. Edgar, G. D. M. Jeffries, and D. T. Chiu, Anal. Chem. **78**, 6433 (2006).
[3]Y. Ai, C. K. Sanders, and B. L. Marrone, Anal. Chem. **85**, 9126 (2013).
[4]J. Guzowski, P. M. Korczyk, S. Jakiela, and P. Garstecki, Lab Chip **11**, 3593 (2011).
[5]J. Hoffmann, M. Plötner, D. Kuckling, and W.-J. Fischer, Sens. Actuators, A **77**, 139 (1999).
[6]S. Haefner, P. Frank, M. Elstner, J. Nowak, S. Odenbach, and A. Richter, Lab Chip **16**, 3977 (2016).
[7]D. Jin, B. Deng, J. X. Li, W. Cai, L. Tu, J. Chen, Q. Wu, and W. H. Wang, Biomicrofluidics **9**, 014101 (2015).
[8]A. Richter, S. Klatt, G. Paschew, and C. Klenke, Lab Chip **9**, 613 (2009).
[9]G. Paschew, J. Schreiter, A. Voigt, C. Pini, J. P. Chávez, M. Allerdißen, U. Marschner, S. Siegmund, R. Schüffny, F. Jülicher, and A. Richter, Adv. Mater. Technol. **1**, 1600005 (2016).
[10]R. Yoshida, K. Uchida, Y. Kaneko, K. Sakai, A. Kikuchi, Y. Sakurai, and T. Okano, Nature **374**, 240 (1995).
[11]E. C. Cho, J.-W. Kim, A. Fernández-Nieves, and D. A. Weitz, Nano Lett. **8**, 168 (2008).
[12]A. B. Imran, T. Seki, and Y. Takeoka, Polym. J. **42**, 839 (2010).
[13]M. Arotçaréna, B. Heise, S. Ishaya, and A. Laschewsky, J. Am. Chem. Soc. **124**, 3787 (2002).
[14]G. H. Kwon, G. S. Jeong, J. Y. Park, J. H. Moon, and S.-H. Lee, Lab Chip **11**, 2910 (2011).
[15]E. Sato Matsuo and T. Tanaka, J. Chem. Phys. **89**, 1695 (1988).
[16]H. Hirose and M. Shibayama, Macromolecules **31**, 5336 (1998).
[17]X.-Z. Zhang, X.-D. Xu, S.-X. Cheng, and R.-X. Zhuo, Soft Matter **4**, 385 (2008).
[18]G. H. Kwon, J. Y. Park, J. Y. Kim, M. L. Frisk, D. J. Beebe, and S.-H. Lee, Small **4**, 2148 (2008).
[19]L. Ionov, Adv. Funct. Mater. **23**, 4555 (2013).
[20]N. Annabi, J. W. Nichol, X. Zhong, C. Ji, S. Koshy, A. Khademhosseini, and F. Dehghani, Tissue Eng. Part B **16**, 371 (2010).
[21]D. Grafe, S. Zschoche, D. Appelhans, and B. Voit, RSC Adv. **6**, 34809 (2016).
[22]L.-W. Xia, R. Xie, X.-J. Ju, W. Wang, Q. Chen, and L.-Y. Chu, Nat. Commun. **4**, 2226 (2013).
[23]E. Wang, M. S. Desai, and S.-W. Lee, Nano Lett. **13**, 2826 (2013).
[24]Y. Kaneko, K. Sakai, A. Kikuchi, R. Yoshida, Y. Sakurai, and T. Okano, Macromolecules **28**, 7717 (1995).
[25]F. Di Lorenzo and S. Seiffert, Polym. J. **6**, 5515 (2015).
[26]R. Luo, J. Wu, N.-D. Dinh, and C.-H. Chen, Adv. Funct. Mater. **25**, 7272 (2015).
[27]R. Luo and C.-H. Chen, Chem. Commun. **51**, 6617 (2015).
[28]S.-Y. Park, T.-H. Wu, Y. Chen, M. A. Teitell, and P.-Y. Chiou, Lab Chip **11**, 1010 (2011).
[29]A. Diguet, H. Li, N. Queyriaux, Y. Chen, and D. Baigl, Lab Chip **11**, 2666 (2011).
[30]J. C. Brenker, D. J. Collins, H. Van Phan, T. Alan, and A. Neild, Lab Chip **16**, 1675 (2016).
[31]Z. Z. Chong, S. H. Tan, A. M. Gañán-Calvo, S. B. Tor, N. H. Loh, and N.-T. Nguyen, Lab Chip **16**, 35 (2016).
[32]R. Lin, J. S. Fisher, M. G. Simon, and A. P. Lee, Biomicrofluidics **6**, 024103 (2012).
[33]J.-Y. Hong, H. Yoon, and J. Jang, Small **6**, 679 (2010).
[34]S. A. Bencherif, R. W. Sands, D. Bhatta, P. Arany, C. S. Verbeke, D. A. Edwards, and D. J. Mooney, Proc. Natl. Acad. Sci. U. S. A. **109**, 19590 (2012).
[35]S. T. Koshy, T. C. Ferrante, S. A. Lewin, and D. J. Mooney, Biomaterials **35**, 2477 (2014).
[36]K. Ren, J. Zhou, and H. Wu, Acc. Chem. Res. **46**, 2396 (2013).
[37]N. S. Satarkar, D. Biswal, and J. Z. Hilt, Soft Matter **6**, 2364 (2010).
[38]P. Paradiso, V. Chu, L. Santos, A. P. Serro, R. Colaço, and B. Saramago, J. Biomed. Mater. Res. Part B **103**, 1059 (2015).
[39]W. Hilber, Appl. Phys. A **122**, 751 (2016).
[40]Z. Zha, X. Yue, Q. Ren, and Z. Dai, Adv. Mater. **25**, 777 (2013).